

# Constraint on Einstein-Gauss-Bonnet Gravity from Neutron Stars

Juan M. Z. Pretel<sup>1,\*</sup> and Ayan Banerjee<sup>2,†</sup>

<sup>1</sup> *Instituto de Física, Universidade Federal do Rio de Janeiro,  
CEP 21941-972 Rio de Janeiro, RJ, Brazil*

<sup>2</sup> *Astrophysics and Cosmology Research Unit, School of Mathematics, Statistics and Computer Science,  
University of KwaZulu-Natal, Private Bag X54001, Durban 4000, South Africa*

(Dated: July 9, 2021)

Within the framework of Einstein-Gauss-Bonnet theory in five-dimensional spacetime (5D EGB), we derive the hydrostatic equilibrium equations and solve them numerically to obtain the neutron stars for both isotropic and anisotropic distribution of matter. The mass-radius relations are obtained for SLy equation of state, which describes both the solid crust and the liquid core of neutron stars, and for a wide range of the Gauss-Bonnet coupling parameter  $\alpha$ . More specifically, we find that the contribution of the Gauss-Bonnet term leads to substantial deviations from the Einstein gravity. We also discuss that after a certain value of  $\alpha$ , the theory admits higher maximum masses compared with general relativity, however, the causality condition is violated in the high-mass region. Finally, our results are compared with the recent observations data on mass-radius diagram.

## I. INTRODUCTION

Einstein's General Relativity (GR) is one of the most successful gravity theories, even after almost one hundred years, that passes successfully with high accuracy all local observational tests both for weak and strong gravity regime [1]. Although successful in describing the observational and the experimental data, there are several unresolved issues which led to an extensive search for alternative gravity theories. In this direction the higher curvature gravity theories are wonderful tools to explore physics beyond the standard model. Their philosophy is based on the metric modification of gravity that generalizes GR in higher dimensions. In particular, Lovelock gravity theories [2, 3] are fascinating extensions of GR that include higher curvature interactions while keeping the order of the field equations down to second order in derivatives. Furthermore, this theory is known to be free of ghosts [4, 5] when expanded on a flat space and obeys generalized Bianchi identities which ensure energy conservation.

We will focus our attention on the Einstein-Gauss-Bonnet (EGB) theory of gravity, whose action is given by the Einstein-Hilbert term plus the cosmological constant term  $\Lambda$ , and both supplemented with the Gauss-Bonnet (GB) term, quadratic in the curvature. Such theory is also known to be most general metric torsion-free theory of gravity which leads to conserved equations of motion. In fact, the GB term naturally arises as a low energy effective action of heterotic string theory [6, 7]. Interestingly the GB term is a topological invariant in 4D spacetime, and hence does not contribute to the gravitational dynamics. Nevertheless, to get a non-trivial contribution, one can generally associate the GB term with the scalar field [8, 9].

Since then EGB gravity theories have been studied by many authors over a wide span of years. In particular, Boulware and Deser [10] first presented spherically symmetric static black hole solution within the frame of the EGB gravity. In Ref. [11] the thermodynamic properties associated with black hole horizon and cosmological horizon have been studied for the GB solution in de Sitter space. Later on several black hole solutions and their interesting properties have been intensively cultivated by several authors, see e.g. Refs. [12–16]. In addition to this many fascinating phenomena such as gravitational collapse of an incoherent spherical dust cloud [17–20], geodesic motion of a test particle [21], the phase transition of RN-AdS black holes [22], radius of photon spheres [23], regular black hole solutions [24] and wormhole solutions satisfying the energy conditions [25, 26] have been well studied in those literatures. Moreover, some models related to compact objects have been studied in Refs. [27–31].

On the other hand, when testing alternative theories one may start from strong-field regime [32]. With this point of view the formation and the evolution of stars can be considered suitable test-beds for higher curvature gravity theory. Thus, neutron stars (NSs), one of the most extreme states of matter found in the Universe, are ideal astrophysical environments to constrain gravity on strong-field regime. The matter in the inner core of NSs is compressed to densities several times higher than the density of an ordinary atomic nuclei. However, the behavior of matter at ultrahigh densities and temperatures are not fully understood of NSs because such high densities cannot be reproduced in the laboratory conducted on Earth. Only theoretical models and methods can be formulated where there are a very large number of EoS candidates.

On the other have, recent measurements of two pulsar masses yielded values close to  $2M_{\odot}$  including the binary millisecond pulsar J1614-2230 [33, 34] and the pulsar J0348+0432 [35], which have provided an important constraint on the EoS at  $\rho \gtrsim \rho_{\text{nuc}}$  where  $\rho_{\text{nuc}} = 2.8 \times 10^{14}$

\*Electronic address: juanzarate@if.ufrj.br

†Electronic address: ayanbanerjeemath@gmail.com

$g/\text{cm}^3$ , and tell us about crucial importance of strong interactions in dense matter physics. Furthermore, the mass-radius ( $M - r_{\text{sur}}$ ) relations of NSs are very useful because they allow us to understand the complex physical phenomena occurring inside such compact astrophysical objects. A large enough set of  $M - r_{\text{sur}}$  measurements is required to determine their influence on other physical properties such as compactness, moment of inertia, spin periods of rotation, among other astrophysical observables [36, 37]. However, extensions of GR can have a substantial impact on the macro-physical properties of a neutron star (see e.g. Ref [38] for a broad review). In spite of that, there is a growing interest not only in restricting the EoS but also in considering viable theories of modified gravity when we study compact stars. It is evident that the EoS and the framework of modified gravity must be constrained from astronomical observations, as for example from multi-messenger observations of the merger GW170817 [39–44].

Although it is very common to adopt isotropic perfect fluids to describe the structure of compact stars, there are strong arguments indicating that the effects of anisotropy cannot be neglected when we deal with nuclear matter at very high densities and pressures (see e.g. Refs. [45–56] and references therein). The presence of anisotropic fluid may lead to significant changes in the characteristics of relativistic stars even in modified gravity as demonstrated in Refs. [57, 58]. Concerning this, some authors [59] have investigated the noteworthy solutions for quark stars in background of EGB theory. The main goal of the present research is to examine the possibility of using the anisotropy to obtain configurations constructed with SLy EoS [60] and to satisfy the current observational data on the  $M - r_{\text{sur}}$  relation. Furthermore, we compare our results with the well measured masses of some massive neutron stars reported in the literature such as the millisecond pulsars PSR J1614-2230 [33] and PSR J0740+6220 [61].

The plan of this paper is the following: In Sect. II we briefly summarize EGB gravity in five dimensions and present the modified TOV equations for stellar structure of anisotropic compact stars. Section III presents the EoS and two anisotropy models that we use to describe anisotropic neutron stars. In Sect. IV we show our numerical results and analyze the deviations of the physical quantities with respect to standard GR. Finally, in Sect. V we provide our conclusions. We adopt physical units throughout this work.

## II. MODIFIED TOV EQUATIONS IN EGB GRAVITY

Our paper begins with the action of  $D$ -dimensional Einstein-Gauss-Bonnet (EGB) theory minimally coupled to matter fields, which reads:

$$S = \frac{1}{2\kappa} \int d^D x \sqrt{-g} [R - 2\Lambda + \alpha\mathcal{G}] + S_m, \quad (1)$$

where  $\kappa \equiv 8\pi G/c^4$ ,  $\Lambda$  is the cosmological constant,  $\alpha$  is the GB coupling constant<sup>1</sup>,  $S_m$  stands for the action of standard matter, and the Gauss-Bonnet invariant  $\mathcal{G}$  is given by

$$\mathcal{G} = R^2 - 4R_{\mu\nu}R^{\mu\nu} + R_{\mu\nu\sigma\rho}R^{\mu\nu\sigma\rho}. \quad (2)$$

We obtain the corresponding field equations by varying the action (1) with respect to metric, which yield

$$G_{\mu\nu} + \alpha H_{\mu\nu} = \kappa T_{\mu\nu}, \quad (3)$$

with  $G_{\mu\nu}$  being the usual Einstein tensor,  $H_{\mu\nu}$  the Gauss-Bonnet tensor, and  $T_{\mu\nu}$  is the energy-momentum tensor of matter. Such tensor quantities are given by

$$G_{\mu\nu} = R_{\mu\nu} - \frac{1}{2}Rg_{\mu\nu}, \quad (4)$$

$$H_{\mu\nu} = 2[RR_{\mu\nu} - 2R_{\mu\sigma}R^{\sigma}_{\nu} - 2R_{\mu\sigma\nu\rho}R^{\sigma\rho} - R_{\mu\sigma\rho\lambda}R^{\sigma\rho\lambda}_{\nu}] - \frac{1}{2}g_{\mu\nu}\mathcal{G}, \quad (5)$$

$$T_{\mu\nu} = -\frac{2}{\sqrt{-g}} \frac{\delta(\sqrt{-g}\mathcal{S}_m)}{\delta g^{\mu\nu}}, \quad (6)$$

where  $R$  is the Ricci scalar,  $R_{\mu\nu}$  the Ricci tensor, and  $R_{\mu\nu\sigma\rho}$  is the Riemann tensor. It is easy to see that for  $\alpha = 0$ , Eq. (3) reduces to the conventional Einstein field equation. Moreover, the GB term does not contribute to the field equations (3) for  $D \leq 4$ .

In order to construct non-rotating neutron stars, the spherically symmetric  $D$ -dimensional metric describing the interior spacetime is written in the form

$$ds_D^2 = -e^{2\psi}(cdt)^2 + e^{2\lambda}dr^2 + r^2 d\Omega_{D-2}^2, \quad (7)$$

where the metric functions  $\psi$  and  $\lambda$  depend only on the radial coordinate  $r$ , and  $d\Omega_{D-2}^2$  represents the metric on the surface of the  $(D-2)$ -sphere, namely

$$d\Omega_{D-2}^2 = d\theta_1^2 + \sin^2\theta_1 d\theta_2^2 + \sin^2\theta_1 \sin^2\theta_2 d\theta_3^2 + \dots + \left( \prod_{j=1}^{D-3} \sin^2\theta_j \right) d\theta_{D-2}^2. \quad (8)$$

In addition, we assume that the matter source is described by an anisotropic fluid, whose energy-momentum tensor is given by

$$T_{\mu\nu} = (\epsilon + p_t)u_\mu u_\nu + p_t g_{\mu\nu} - \sigma k_\mu k_\nu, \quad (9)$$

with  $u^\mu$  being the  $D$ -velocity of the fluid,  $\epsilon = c^2\rho$  the energy density of standard matter,  $\rho$  the mass density,  $p_r$  the radial pressure,  $p_t$  the tangential pressure,  $\sigma \equiv p_t - p_r$  the anisotropy factor, and  $k^\mu$  is a unit spacelike  $D$ -vector along the radial coordinate.

<sup>1</sup> This constant has dimensions of length squared and is related to the string tension in string theory.

For the line element (7) and energy-momentum tensor (9), the  $tt$  and  $rr$  components of the field equations (3) are given by [59]

$$\frac{2}{r} \frac{\lambda'}{e^{2\lambda}} = \left\{ \frac{2\kappa\epsilon}{D-2} - \frac{1-e^{-2\lambda}}{r^2} [(D-3) + \frac{\alpha}{r^2}(D-5)(1-e^{-2\lambda})] \right\} \left[ 1 + \frac{2\alpha}{r^2}(1-e^{-2\lambda}) \right]^{-1}, \quad (10)$$

$$\frac{2}{r} \frac{\psi'}{e^{2\lambda}} = \left\{ \frac{2\kappa p_r}{D-2} + \frac{1-e^{-2\lambda}}{r^2} [(D-3) + \frac{\alpha}{r^2}(D-5)(1-e^{-2\lambda})] \right\} \left[ 1 + \frac{2\alpha}{r^2}(1-e^{-2\lambda}) \right]^{-1}, \quad (11)$$

where the prime denotes differentiation with respect to the radial coordinate  $r$ . It is now evident that there is an extra contribution due to higher order terms for  $D \geq 5$ . Here we assume the particular case  $D = 5$ , where the quadratic extensions are nontrivial for the stellar structure. Consequently, within the framework of 5D EGB gravity, Eq. (10) leads to an analogous expression as in GR, namely

$$\frac{d}{dr}(re^{-2\lambda}) - 1 = -\kappa r^2 c^2 \rho_{\text{tot}}, \quad (12)$$

where  $\rho_{\text{tot}}$  can be interpreted as a total mass density, given by

$$\rho_{\text{tot}} \equiv \frac{2}{3}\rho + \frac{e^{-2\lambda} - 1}{\kappa c^2 r^2} \left[ 1 + \frac{4\alpha}{r} \lambda' e^{-2\lambda} \right]. \quad (13)$$

To recast these equations into a more familiar form let us now introduce a mass function  $m(r)$  through the following relation

$$e^{-2\lambda} = 1 - \frac{2Gm}{c^2 r}, \quad (14)$$

which can be obtained from the integration of Eq. (12). Thus, the total gravitational mass enclosed by a sphere of radius  $r$  can be written as

$$m(r) = 4\pi \int_0^r \bar{r}^2 \rho_{\text{tot}}(\bar{r}) d\bar{r}. \quad (15)$$

For a static spherical fluid ball, the energy-momentum conservation equation is given by  $\nabla_\mu T^{\mu\nu} = 0$ , which leads to

$$\frac{d\psi}{dr} = -\frac{1}{c^2 \rho + p_r} \frac{dp_r}{dr} + \frac{3\sigma}{r(c^2 \rho + p_r)}. \quad (16)$$

Accordingly, by taking into account the field equations (10) and (11) for  $D = 5$  together with Eqs. (14) and (16), we find that the modified Tolman-Oppenheimer-Volkoff

(TOV) equations for 5D EGB gravity, now read

$$\frac{dm}{dr} = \left[ \frac{8\pi}{3} r^6 \rho - r^3 m + \frac{4\alpha G}{c^2} m^2 \right] \left[ r^4 + \frac{4\alpha G}{c^2} r m \right]^{-1}, \quad (17)$$

$$\frac{dp_r}{dr} = -2G \left[ \frac{c^2 \rho + p_r}{c^2} \right] \left[ \frac{m}{r^2} + \frac{4\pi}{3c^2} r p_r \right] \times \left[ 1 + \frac{4\alpha G m}{c^2 r^3} \right]^{-1} \left[ 1 - \frac{2Gm}{c^2 r} \right]^{-1} + \frac{3}{r} \sigma. \quad (18)$$

In other words, Eqs. (17) and (18) are the hydrostatic equilibrium equations for relativistic stars in 5D EGB gravity. It is clear that by setting  $\alpha$  to zero, these equations reduce to the conventional TOV equations. In order to close the system, an EoS  $p_r = p_r(\rho)$  and a specific anisotropy relation for  $\sigma$  are required. This enables one to impose the following boundary conditions

$$\rho(0) = \rho_c, \quad m(0) = 0, \quad (19)$$

i.e., Eqs. (17) and (18) can be integrated for a given central mass density and maintaining the regularity conditions at the center of the star. It is evident that when anisotropy vanishes i.e.,  $\sigma = 0$ , the above system of equations is reduced to the isotropic case.

### III. EQUATION OF STATE AND ANISOTROPY PROFILE

As already mentioned before, to close the system of modified TOV equations and therefore determine the global properties of a NS, it is required to choose an EoS for the micro-physics of dense matter. Although it was initially hypothesized that NSs contain mainly neutrons as if they were a Fermi gas, nowadays we know that the nature and composition of matter in the high-density inner cores of such objects is still unknown. In fact, there are a large number of theoretical models that differ in assumptions about composition, symmetry energy, multi-body interactions, among other inputs [37, 62]. Here we will employ an EoS that involves only nucleonic matter.

In order to construct anisotropic NSs in 5D EGB gravity, we follow a procedure analogous to that carried out in Einstein gravity. Namely, one needs to specify a barotropic EoS for radial pressure and also assign an anisotropy function  $\sigma \equiv p_t - p_r$  since there is an extra degree of freedom. Nonetheless, it is worth noting that some authors have adopted an EoS for both radial and tangential pressure, see e.g. Refs. [63, 64] for discussions on the matter.

For the micro-physical relation between mass density and radial pressure of stellar fluid, we use the well-known SLy EoS [60] which is compatible with the constraints extracted from the event GW170817 — the first detection of gravitational waves from a binary neutron star inspiral [65]. This unified EoS describes both the thin crust and

the massive liquid core of NSs, and it can be represented by the following equation [66]

$$\begin{aligned} \zeta(\xi) = & \frac{a_1 + a_2\xi + a_3\xi^3}{1 + a_4\xi} f(a_5(\xi - a_6)) \\ & + (a_7 + a_8\xi)f(a_9(a_{10} - \xi)) \\ & + (a_{11} + a_{12}\xi)f(a_{13}(a_{14} - \xi)) \\ & + (a_{15} + a_{16}\xi)f(a_{17}(a_{18} - \xi)), \end{aligned} \quad (20)$$

where  $\zeta \equiv \log(p_r/\text{dyn cm}^{-2})$ ,  $\xi \equiv \log(\rho/g \text{ cm}^{-3})$  and  $f(x) \equiv 1/(e^x + 1)$ , respectively. The values  $a_i$  are fitting parameters and can be found in Ref. [66]. Besides this EoS, we employ two anisotropy profiles for  $\sigma$  provided in the literature to model anisotropic matter at very high densities and pressures. In what follows we will describe in more detail the functional relations for the anisotropy.

The first anisotropy profile adopted in this work is the model proposed by Horvat *et al* in Ref. [67], given by

$$\sigma = \beta_{\text{H}} p_r \mu = \beta_{\text{H}} p_r (1 - e^{-2\lambda}), \quad (21)$$

where  $\beta_{\text{H}}$  is a dimensionless parameter that measures the amount of anisotropy inside the star and, in principle, it can assume positive or negative values of the order of unity [47, 48, 54, 57, 68, 69]. Such anisotropy model is also known as quasi-local ansatz because the compactness  $\mu$  denotes a quasi-local variable. Since  $\mu \rightarrow 0$  when  $r \rightarrow 0$ , the relation (21) guarantees that the anisotropy factor vanishes at the stellar center, i.e. the fluid becomes isotropic. Furthermore, in the Newtonian limit (when the pressure contribution to the energy density is negligible) the effect of anisotropy vanishes in the hydrostatic equilibrium equation.

Following Bowers and Liang [70], we will consider another form of the anisotropy factor,

$$\sigma = \frac{\beta_{\text{BL}} G}{c^4} (c^2 \rho + p_r)(c^2 \rho + 3p_r) e^{2\lambda} r^2, \quad (22)$$

for a non-rotating configuration. Here,  $\beta_{\text{BL}}$  is a constant parameter that quantifies the amount of anisotropy, and we recover the isotropic case when  $\beta_{\text{BL}} = 0$ . Moreover, in the non-relativistic regime the effect of anisotropy does not vanish in the hydrostatic equilibrium equation, which could be an unphysical trait as argued in Ref. [69]. The anisotropy parameter  $\beta_{\text{BL}}$  assumes values similar to  $\beta_{\text{H}}$  [48, 54, 57, 68, 69, 71].

## IV. NUMERICAL RESULTS AND DISCUSSION

### A. Isotropic configurations

Let us begin by examining the isotropic case (i.e., when  $p_t = p_r = p$ ) within the context of 5D EGB gravity. To do so, we numerically integrate the modified TOV equations (17) and (18) with boundary conditions (19) from the center at  $r = 0$  up to the stellar surface at  $r = r_{\text{sur}}$  where the pressure vanishes. In addition, we

TABLE I: Isotropic NSs with central mass density  $\rho_c = 2.0 \times 10^{18} \text{ kg/m}^3$  corresponding SLy EoS in 5D EGB gravity for different values of the coupling constant. The corresponding graphs for mass function and pressure are plotted in Fig. 1. The difference in mass between the values obtained in GR (in 4D) and 5D EGB gravity is given by  $\Delta M$ .

Theory: $\alpha$ [km <sup>2</sup> ]	$r_{\text{sur}}$ [km]	$M$ [ $M_{\odot}$ ]	$\Delta M$ [ $M_{\odot}$ ]
-10	12.827	1.239	0.751
-5	13.044	1.330	0.660
0	13.256	1.418	0.572
5	13.463	1.504	0.486
10	13.664	1.587	0.403
20	14.047	1.746	0.244

set  $\sigma = 0$  and specify a value for the coupling constant  $\alpha$ . In particular, for a central mass density  $\rho_c = 2.0 \times 10^{18} \text{ kg/m}^3$  with SLy EoS (20), we obtain the solutions shown in Fig. 1. This figure shows typical values for the star's mass  $M \sim (1.2 - 1.7) M_{\odot}$  corresponding to their isotropic pressure. As one can see the properties of such stars change considerably when we vary the parameter  $\alpha$ . Indeed, as  $\alpha$  increases the surface radius and total mass of the star also increases. In Table I, we show how much the mass obtained in EGB gravity varies with respect to its corresponding GR value. It is noticeable that for a given value of  $\alpha$  in the left plot of Fig. 1, the mass function suffers a small drop after reaching a maximum value near the surface. This phenomenon associated with only the EGB gravity not their standard GR counterparts where the mass function is always increasing as we approach the surface of the star.

By solving the stellar structure equations for a range of central density values, we can get a family of NSs in 5D EGB gravity. Figure 2 illustrates the mass-radius and mass-central density relations for the SLy nucleonic EoS and different values of  $\alpha$ . We also showed that for the case of GR a smaller central density yields a less massive NS and would lead to less compact object. In this perspective, the GB term plays an important role for EGB theory of gravity identifying a substantial deviation on  $M - r_{\text{sur}}$  relations at which EGB results differ significantly from standard GR in 4D.

The maximum-mass points on the mass versus central density curves can even exceed the GR counterpart from a certain value of the coupling constant. Nevertheless, according to the right panel of Fig. 2, we see that there is a region where the speed of sound (defined by  $c_s \equiv \sqrt{dp/d\rho}$ ) is greater than the speed of light  $c$ . This violates the causality condition, and thus it is not possible to describe physically realistic massive NSs in EGB gravity considering only isotropic pressures.

On the other hand, the stellar configurations presented in Fig. 2 describe NSs in hydrostatic equilibrium, however, such equilibrium can be stable or unstable with respect to a small radial perturbation. It has been shown, at least in GR (see e.g. Refs. [72, 73]), that a

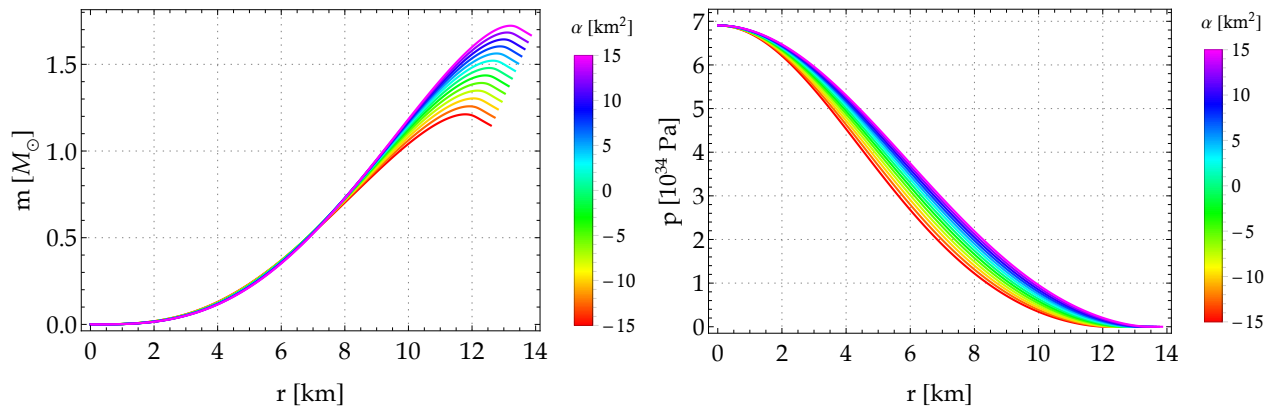


FIG. 1: Mass parameter (left panel) and pressure of the isotropic fluid (right panel) as functions of the radial coordinate within the framework of  $5D$  EGB theory of gravity. These plots correspond to a central mass density  $\rho_c = 2.0 \times 10^{18} \text{ kg/m}^3$  with SLy EoS (20) for  $\sigma = 0$  and different values of the coupling constant  $\alpha$ . The gravitational mass (at the surface) of the star increases with increasing value of  $\alpha$ . Interestingly, the mass suffers a small drop after reaching a maximum near the surface for any value of  $\alpha$ . For some specific calculations of surface radius and mass, see also Table I.

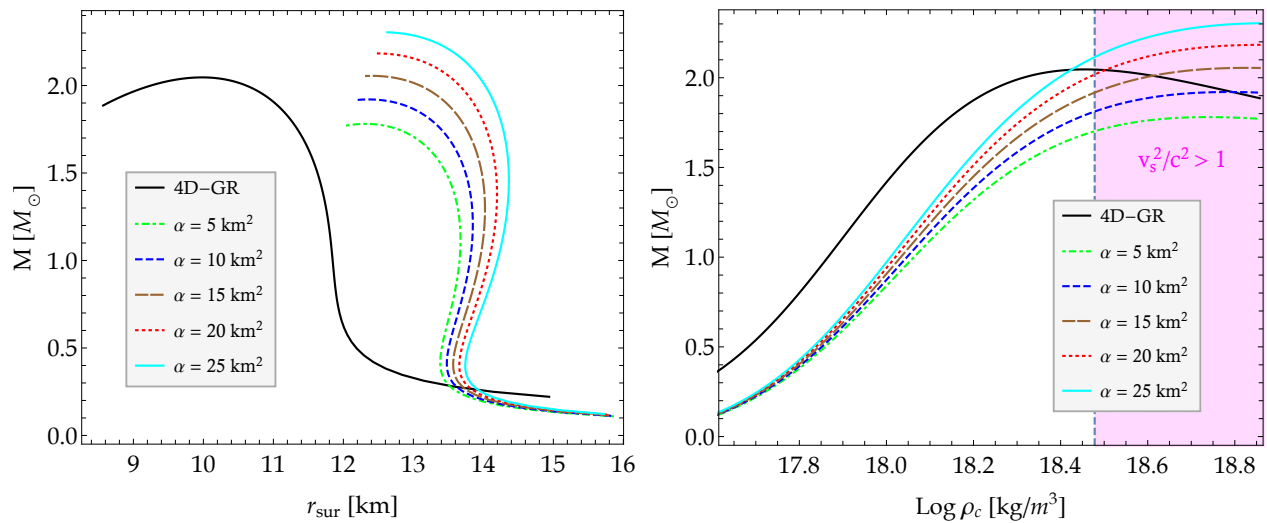


FIG. 2: Left panel: Mass-radius diagram in  $5D$  EGB gravity for several values of  $\alpha$ , where  $M$  represents the total gravitational mass on the surface of the star. Right panel: Mass-central density relation, where the magenta region indicates that the sound speed is greater than the speed of light in neutron-star matter with SLy EoS. The standard GR solution is shown in both plots as a benchmark by a solid black line. Note that the solutions corresponding to the EGB gravity generate maximum-mass configurations that do not satisfy the causality condition at the stellar center.

turning point from stability to instability occurs when  $dM(\rho_c)/d\rho_c = 0$ . This means that the stable branch in the sequence of stars is located before the critical density corresponding to the maximum-mass point. Consequently, the stable stars in the right panel of Fig. 2 are found in the region where  $dM(\rho_c)/d\rho_c > 0$ . Due to its simplicity, this condition has been widely used in the literature. Nevertheless, we must point out that such a condition is just necessary but not sufficient to determine the limits of stellar stability. A more rigorous analysis about the radial stability of such stars will be left for future work.

It is known in GR that the existence of anisotropic pressure leads to more massive compact stars. Thus in

TABLE II: Measurements of masses for the most massive neutron stars observed in nature.

Source and reference	Measured mass [ $M_\odot$ ]
PSR J1614-2230 [33]	$1.97 \pm 0.04$
PSR J0348+0432 [35]	$2.01 \pm 0.04$
PSR J0740+6620 [61]	$2.14^{+0.10}_{-0.09}$
PSR 2215+5135 [74]	$2.27^{+0.17}_{-0.15}$

the next section we are going to explore the consequences of including anisotropy in the stellar structure within the framework of  $5D$  EGB gravity.

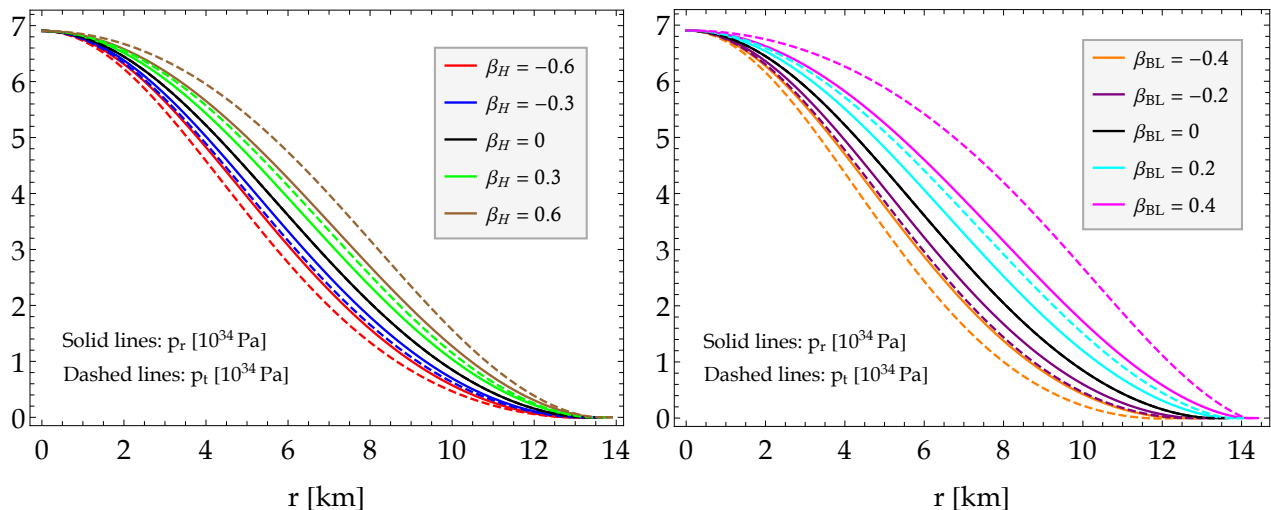


FIG. 3: Numerical solution of the system of equations (17) and (18) for a NS with central density  $\rho_c = 2.0 \times 10^{18} \text{ kg/m}^3$  and SLy EoS in 5D EGB gravity with  $\alpha = 10 \text{ km}^2$  for both plots. We used the quasi-local ansatz (left panel) and Bowers-Liang profile (right panel) for different values of the anisotropy parameters  $\beta_H$  and  $\beta_{BL}$ . The solid and dashed curves correspond to the radial and tangential pressures, respectively. For each profile, larger values of  $|\beta|$  correlate with higher amounts of anisotropy in the intermediate regions of the star. We also note that the anisotropy vanishes both at the center and at the surface of the star, as expected.

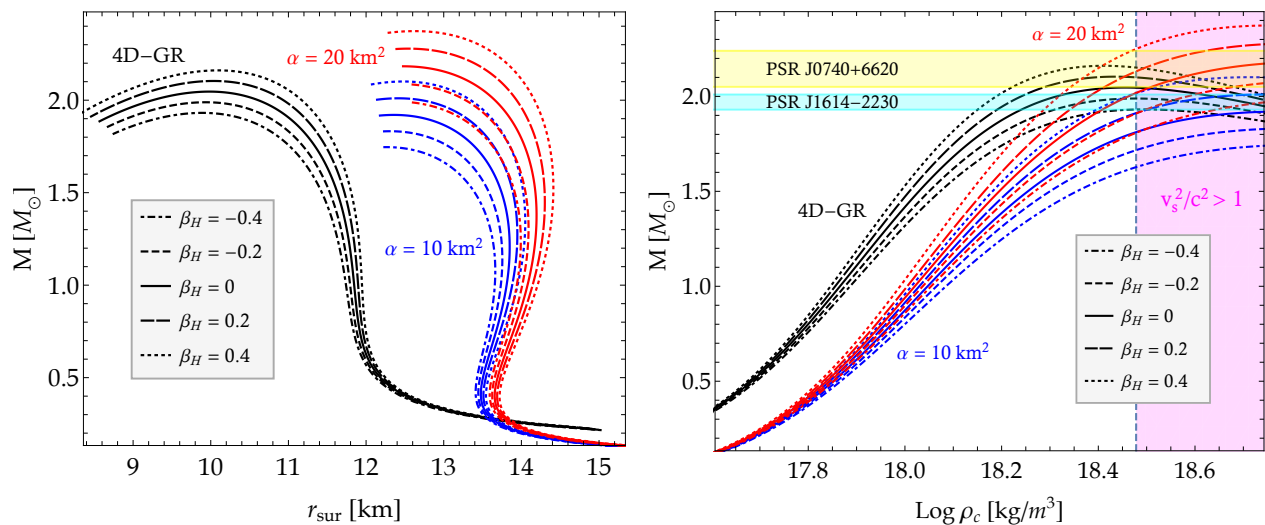


FIG. 4: Illustration of the macro-physical properties predicted by the 5D EGB gravity. Mass versus radius curves (left panel) and mass versus central density relations (right panel) for anisotropic NSs with SLy EoS for radial pressure and anisotropy profile (21). The standard GR solution has been included for comparison reasons. As we can see, both radius and mass undergo significant changes due to the influence of the GB term as well as the anisotropy parameters  $\beta_H$ . The horizontal bands in cyan and yellow colors stand for the observational measurements of the NS masses reported in Refs. [33] and [61], respectively. The magenta region indicates that  $c_s^2 \equiv dp_r/d\rho > c^2$  at the stellar center.

## B. Anisotropic configurations

Bearing in mind that our aim is also to explore the effect of pressure anisotropy on NSs, here we include an anisotropy factor  $\sigma$  in the TOV equations. In other words, we numerically solve the system of Eqs. (17) and (18) by setting the boundary conditions (19), and specifying the values of coupling constant  $\alpha$  as well as the

anisotropy parameter  $\beta$ . We use the anisotropy profiles (21) with  $\beta_H$  and (22) with  $\beta_{BL}$ , where the tangential pressure  $p_t$  differs from the radial one  $p_r$  through an ansatz. For each model under consideration, the isotropic case can be recovered when  $\beta \rightarrow 0$ .

The radial profile of each model is illustrated in the plots of Fig. 3 for a central density  $\rho_c = 2.0 \times 10^{18} \text{ kg/m}^3$ ,  $\alpha = 10 \text{ km}^2$ , and for several values of  $\beta$ . Each color in-

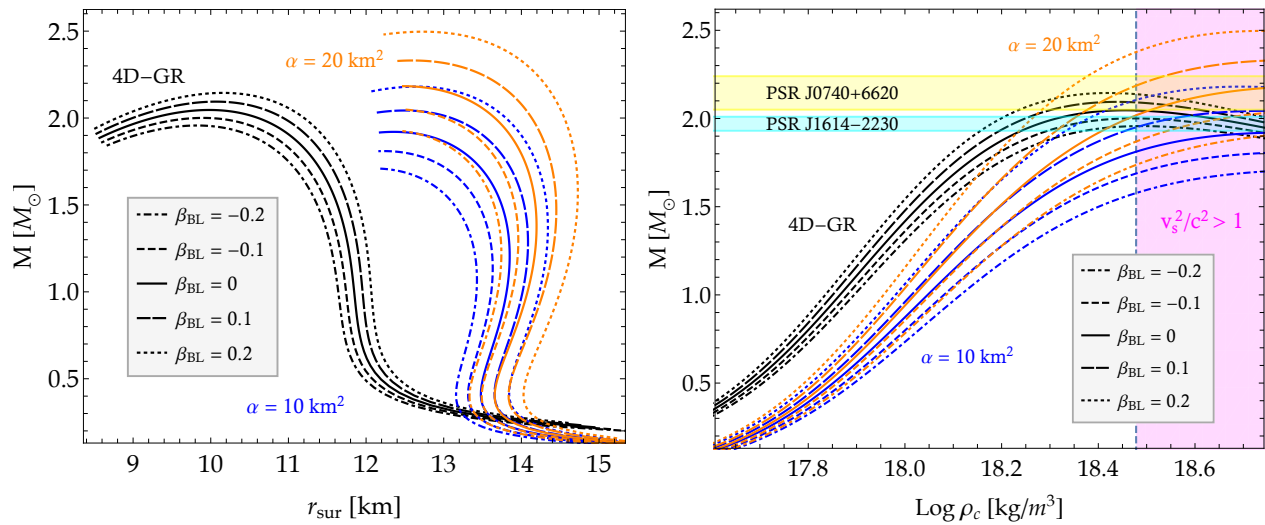


FIG. 5: Mass-radius diagrams (left panel) and mass-central density relations (right panel) for anisotropic neutron stars in 5D EGB gravity with anisotropy profile (22). Note that the behavior in the curves is qualitatively similar to the results of Fig. 4, although the values of  $\beta_{BL}$  are smaller than  $\beta_H$ . Furthermore, at low central densities, the quasi-local ansatz introduces greater changes in the gravitational mass than the Bowers-Liang ansatz. The colored regions represent the same as in Fig. 4.

indicates a specific value of the anisotropy parameter, and solid and dashed lines stand for radial and tangential pressure, respectively. It is interesting to observe that for the two models adopted here the anisotropy vanishes at the center (which is a required condition in order to guarantee regularity), is highest in the intermediate regions, and it vanishes again at the stellar surface. These results reveal that anisotropies have a similar qualitative behaviour for both ansatz.

For the anisotropy function (21), Fig. 4 displays the mass-radius and mass-central density relations for anisotropic NSs with SLy EoS in EGB gravity for two particular values of the coupling constant  $\alpha$ . It is evident that for lower values of coupling constant the maximum masses and their corresponding maximum radius have lower values, which is similar to the isotropic case. Nonetheless, the anisotropy parameter  $\beta_H$  introduces relevant changes in both mass and radius, mainly in the high-central-density region. Positive (negative) values of  $\beta_H$  generate higher (lower) maximum masses with respect to the isotropic case. This means that the higher-order curvature terms (i.e., the quadratic GB term) and the influence of anisotropies give rise to massive NSs whose results are in good agreement with the observational constraints on millisecond pulsar that coming from different astrophysical sources. Finally, in Table II, we present the numerical values for the systems under consideration and show that our results are consistent with the recent observational data. However, once again we have to point out that the maximum-mass configurations are found in the region where the causality condition is violated.

Finally, in Figure 5, we demonstrate the mass-radius and mass-central density diagrams for the anisotropy profile (22). It can be noted that the behavior is qualitatively similar to the results generated by ansatz (21),

although the values of  $\beta_{BL}$  are smaller than  $\beta_H$ . As a result, an action containing higher-order curvature terms (with suitable values of the parameter  $\alpha$ ) together with the presence of anisotropy allow us to obtain maximum masses greater than  $2.0 M_\odot$ .

## V. CONCLUSIONS

In this work we have studied static neutron stars within the context of 5-dimensional Einstein-Gauss-Bonnet theory of gravity. The GB term (built out of quadratic contractions of the Riemann and Ricci tensors) generates a nontrivial extra contribution that ends up influencing the internal structure of the stars and, consequently, modifies the mass-radius relations. Initially we have obtained numerical solutions corresponding to stellar configurations described by an isotropic fluid where the degree of modification with respect to Einstein gravity is measured by the GB coupling constant  $\alpha$ . Depending on the internal structure of the stars, EGB gravity leads to more compact stars compared with GR. In particular, under a certain value of  $\alpha$ , the radius increases and the gravitational mass decreases. Furthermore, it is possible to obtain larger maximum masses for certain positive values of  $\alpha$ , however, such configurations violate the causality condition.

In addition, we have explored the role of anisotropies in the stellar structure by introducing an extra degree of freedom  $\sigma$  in which the free parameter  $\beta$  is set with the help of some phenomenological ansatz. The parameter  $\beta$  measures the deviation from the isotropic fluid. We have analyzed how the GB term and the fluid anisotropies modify the two most basic properties of NSs. We have shown that the effect of anisotropic pressure is mainly

increasing the mass and radius of the NSs. This finding confirms that NSs are sensitive to the choice of an isotropic model. Thus, our constraints on the maximum NS mass are in good agreement with theoretical calculations and the current observational measurements. Of course, we should remark that this depends on the amount of anisotropy inside the star.

Since, the standard GR does not reveal the existence of super-massive NSs using a soft EoS (for instance, the SLy EoS favored by GW170817), it becomes interesting to explore extensions of Einstein gravity. Concerning this, we have studied how the values of  $\alpha$  and  $\beta$  would affect the gravitational mass of a NS, i.e., how the Gauss-Bonnet Lagrangian and anisotropies would give rise to smaller and larger masses with respect to the GR counterpart. Although several researchers have already investigated the observational restrictions on regularized  $4D$  EGB gravity [75, 76], we expect that future astronomical observations will allow us to impose tight constraints on the coupling constant  $\alpha$  in  $5D$  EGB gravity, also. Us-

ing our inference of the maximum NS mass, one may be able to identify what is the degree of modification with respect to GR.

In future works, it would be interesting to analyze the stability of these stars by calculating the oscillation mode frequencies when the star is subjected to radial perturbations. It is well known that the maximum-mass point indicates the onset of instability, however, this is a necessary but not sufficient condition to determine the limits of stability. In order to fully investigate the stability problem, one would have to solve the perturbed field equations for small radial oscillations from equilibrium.

### Acknowledgments

JMZIP acknowledges Brazilian funding agency CAPES for PhD scholarship 331080/2019.

- 
- [1] C. M. Will, *Living Rev. Relativ.* **17**, 4 (2014).
  - [2] D. Lovelock, *J. Math. Phys.* **12**, 498 (1971).
  - [3] D. Lovelock, *J. Math. Phys.* **13**, 874 (1972).
  - [4] B. Zwiebach, *Physics Letters B* **156**, 315 (1985).
  - [5] B. Zumino, *Physics Reports* **137**, 109 (1986).
  - [6] D. Wiltshire, *Physics Letters B* **169**, 36 (1986).
  - [7] J. T. Wheeler, *Nuclear Physics B* **268**, 737 (1986).
  - [8] S. Odintsov and V. Oikonomou, *Physics Letters B* **805**, 135437 (2020).
  - [9] S. Odintsov, V. Oikonomou, and F. Fronimos, *Nuclear Physics B* **958**, 115135 (2020).
  - [10] D. G. Boulware and S. Deser, *Phys. Rev. Lett.* **55**, 2656 (1985).
  - [11] R.-G. Cai and Q. Guo, *Phys. Rev. D* **69**, 104025 (2004).
  - [12] S. G. Ghosh, M. Amir, and S. D. Maharaj, *European Physical Journal C* **77**, 530 (2017).
  - [13] D. Rubiera-Garcia, *Phys. Rev. D* **91**, 064065 (2015).
  - [14] A. Giacomini, J. Oliva, and A. Vera, *Phys. Rev. D* **91**, 104033 (2015).
  - [15] L. Aránguiz, X.-M. Kuang, and O. Miskovic, *Phys. Rev. D* **93**, 064039 (2016).
  - [16] W. Xu, J. Wang, and X. he Meng, *Physics Letters B* **742**, 225 (2015).
  - [17] S. Jhingan and S. G. Ghosh, *Phys. Rev. D* **81**, 024010 (2010).
  - [18] H. Maeda, *Phys. Rev. D* **73**, 104004 (2006).
  - [19] D. C. Z. K. Zhou, Z. Y. Yang and R. H. Yue, *Mod. Phys. Lett. A* **26**, 2135 (2011).
  - [20] G. Abbas and M. Zubair, *Mod. Phys. Lett. A* **30**, 1550038 (2015).
  - [21] B. Bhawal, *Phys. Rev. D* **42**, 449 (1990).
  - [22] W. Xu, C. y. Wang, and B. Zhu, *Phys. Rev. D* **99**, 044010 (2019).
  - [23] E. Gallo and J. R. Villanueva, *Phys. Rev. D* **92**, 064048 (2015).
  - [24] S. G. Ghosh, D. V. Singh, and S. D. Maharaj, *Phys. Rev. D* **97**, 104050 (2018).
  - [25] H. Maeda and M. Nozawa, *Phys. Rev. D* **78**, 024005 (2008).
  - [26] M. R. Mehdizadeh, M. K. Zangeneh, and F. S. N. Lobo, *Phys. Rev. D* **91**, 084004 (2015).
  - [27] T. Tangphati, A. Pradhan, A. Errehymy, and A. Banerjee, *Annals of Physics* **430**, 168498 (2021).
  - [28] S. D. Maharaj, B. Chilambwe, and S. Hansraj, *Phys. Rev. D* **91**, 084049 (2015).
  - [29] B. C. S. Hansraj and S. D. Maharaj, *Eur. Phys. J. C* **75**, 277 (2015).
  - [30] S. Hansraj, G. Megandhren, A. Banerjee, and N. Mkhize, *Classical and Quantum Gravity* **38**, 065018 (2021).
  - [31] S. Hansraj, S. D. Maharaj, and B. Chilambwe, *Phys. Rev. D* **100**, 124029 (2019).
  - [32] D. Psaltis, *Living Rev. Rel.* **11**, 9 (2008).
  - [33] P. Demorest, T. Pennucci, S. M. Ransom, M. S. E. Roberts, and J. W. T. Hessels, *Nature* **467**, 1081 (2010).
  - [34] E. Fonseca and et al., *The Astrophysical Journal* **832**, 167 (2016).
  - [35] J. Antoniadis and et al., *Science* **340**, 6131 (2013).
  - [36] J. M. Lattimer and M. Prakash, *Physics Reports* **621**, 127 (2016), memorial Volume in Honor of Gerald E. Brown.
  - [37] F. Özel and P. Freire, *Annual Review of Astronomy and Astrophysics* **54**, 401 (2016).
  - [38] G. J. Olmo, D. Rubiera-Garcia, and A. Wojnar, *Physics Reports* **876**, 1 (2020).
  - [39] E. Annala, T. Gorda, A. Kurkela, and A. Vuorinen, *Phys. Rev. Lett.* **120**, 172703 (2018).
  - [40] M. W. Coughlin and et al., *MNRAS* **480**, 3871 (2018).
  - [41] D. Radice, A. Perego, F. Zappa, and S. Bernuzzi, *The Astrophysical Journal* **852**, L29 (2018).
  - [42] P. Creminelli and F. Vernizzi, *Phys. Rev. Lett.* **119**, 251302 (2017).
  - [43] J. M. Ezquiaga and M. Zumalacárregui, *Phys. Rev. Lett.* **119**, 251304 (2017).
  - [44] T. Baker, E. Bellini, P. G. Ferreira, M. Lagos, J. Noller, and I. Sawicki, *Phys. Rev. Lett.* **119**, 251301 (2017).

- [45] L. Herrera and N. Santos, *Physics Reports* **286**, 53 (1997).
- [46] L. Herrera and W. Barreto, *Phys. Rev. D* **88**, 084022 (2013).
- [47] D. D. Doneva and S. S. Yazadjiev, *Phys. Rev. D* **85**, 124023 (2012).
- [48] J. D. Arbañil and M. Malheiro, *JCAP* **2016**, 012 (2016).
- [49] A. A. Isayev, *Phys. Rev. D* **96**, 083007 (2017).
- [50] B. V. Ivanov, *Eur. Phys. J. C* **77**, 738 (2017).
- [51] S. K. Maurya, A. Banerjee, and S. Hansraj, *Phys. Rev. D* **97**, 044022 (2018).
- [52] G. Raposo, P. Pani, M. Bezares, C. Palenzuela, and V. Cardoso, *Phys. Rev. D* **99**, 104072 (2019).
- [53] A. M. Setiawan and A. Sulaksono, *Eur. Phys. J. C* **79**, 755 (2019).
- [54] J. M. Z. Pretel, *Eur. Phys. J. C* **80**, 726 (2020).
- [55] A. Rahmansyah and et al., *Eur. Phys. J. C* **80**, 769 (2020).
- [56] Z. Roupas and G. G. L. Nashed, *Eur. Phys. J. C* **80**, 905 (2020).
- [57] V. Folomeev, *Phys. Rev. D* **97**, 124009 (2018).
- [58] G. Panotopoulos, T. Tangphati, A. Banerjee, and M. Jasim, *Physics Letters B* **817**, 136330 (2021).
- [59] T. Tangphati, A. Pradhan, A. Errehymy, and A. Banerjee, *Physics Letters B* **819**, 136423 (2021).
- [60] F. Douchin and P. Haensel, *A&A* **380**, 151 (2001).
- [61] H. T. Cromartie and et al., *Nature Astronomy* **4**, 72 (2019).
- [62] A. G. Chaves and T. Hinderer, *Journal of Physics G: Nuclear and Particle Physics* **46**, 123002 (2019).
- [63] G. Abellán, E. Fuenmayor, and L. Herrera, *Physics of the Dark Universe* **28**, 100549 (2020).
- [64] G. Abellán, E. Fuenmayor, E. Contreras, and L. Herrera, *Physics of the Dark Universe* **30**, 100632 (2020).
- [65] R. Abbott, et al. (LIGO Scientific, and V. Collaborations), *Phys. Rev. Lett.* **119**, 161101 (2017).
- [66] P. Haensel and A. Y. Potekhin, *A&A* **428**, 191 (2004).
- [67] D. Horvat, S. Ilijić, and A. Marunović, *Classical and Quantum Gravity* **28**, 025009 (2010).
- [68] H. O. Silva, C. F. B. Macedo, E. Berti, and L. C. B. Crispino, *Classical and Quantum Gravity* **32**, 145008 (2015).
- [69] K. Yagi and N. Yunes, *Phys. Rev. D* **91**, 123008 (2015).
- [70] R. L. Bowers and E. P. T. Liang, *Astrophys. J.* **188**, 657 (1974).
- [71] B. Biswas and S. Bose, *Phys. Rev. D* **99**, 104002 (2019).
- [72] N. K. Glendenning, *Compact Stars: Nuclear Physics, Particle Physics, and General Relativity*, 2nd ed. (Astrophys. Library, Springer, New York, 2000).
- [73] P. Haensel, A. Y. Potekhin, and D. G. Yakovlev, *Neutron stars 1: Equation of State and Structure*, 1st ed. (Astrophys. and Space Science Library, Springer, New York, 2007).
- [74] M. Linares, T. Shahbaz, and J. Casares, *Astrophys. J.* **859**, 54 (2018).
- [75] T. Clifton, P. Carrilho, P. G. S. Fernandes, and D. J. Mulryne, *Phys. Rev. D* **102**, 084005 (2020).
- [76] J.-X. Feng, B.-M. Gu, and F.-W. Shu, *Phys. Rev. D* **103**, 064002 (2021).